



Peer review status:

This is a non-peer-reviewed preprint submitted to EarthArXiv.

1

2

3 **Occurrence of tetraester and mixed ether/ester-bound *iso*-diabolic acid membrane-**  
4 **spanning lipids in mineral soils**

5

6 Francien Peterse<sup>1\*</sup>, Klaas G.J. Nierop<sup>1</sup>, Nicole Bale<sup>2</sup>, Sarah Feakins<sup>3</sup>, Chan-Mao Chen<sup>3</sup>

7 <sup>1</sup> Department of Earth Sciences, Utrecht University, Utrecht, the Netherlands

8 <sup>2</sup> Department of Marine Microbiology and Biogeochemistry, Royal NIOZ Netherlands

9 Institute for Sea Research, Texel, the Netherlands

10 <sup>3</sup> Department of Earth Sciences, University of Southern California, Los Angeles, CA, USA

11 \* Corresponding author ([f.peterse@uu.nl](mailto:f.peterse@uu.nl))

12

13

14 *This manuscript is a non-peer reviewed preprint submitted to EarthArXiv. The manuscript has*  
15 *been submitted to Organic Geochemistry.*

16

17

18

19 **Highlights**

- 20 - Mixed ether/ester-bound membrane spanning lipids identified in mineral soils
- 21 - Different compounds released upon hydrolysis suggest distinct synthesis pathways
- 22 - Our findings support both current hypothesized pathways for brGDGT synthesis

23

## 24 **Abstract**

25 Branched glycerol dialkyl glycerol tetraethers (brGDGTs) are a suite of membrane lipids that  
26 are widely used as empirical proxies for past temperature and pH. Although the  
27 stereochemistry of their glycerol moiety suggests that they are produced by bacteria, the  
28 exact producers and the biosynthetic pathway of brGDGTs remain unclear. Here we report  
29 the occurrence of tetraester and mixed ester/ether membrane-spanning lipids with a  
30 backbone consisting of *iso*-diabolic acid (*iso*-DA) containing up to two additional methyl  
31 groups in mineral soils from Nepal and Rwanda. These compounds are presumed  
32 intermediate products during brGDGT synthesis but had not been detected in cultures or the  
33 environment before. Interestingly, while acid hydrolysis of the polar fraction releases *iso*-DA  
34 in the soil from Nepal, monoalkyl glycerol ethers with *iso*-C<sub>15</sub> and *iso*-C<sub>17</sub> chains are released  
35 in the soil from Rwanda. These results support both current hypotheses that brGDGT  
36 synthesis can occur via tail-to-tail condensation of two *iso*-C<sub>15</sub> fatty acids to form *iso*-DA, as  
37 well as through the reduction of diesters to diethers and subsequent carbon-carbon linking  
38 as shown to occur during the synthesis of archaeal GDGTs.

39

40 **Keywords:** branched GDGTs, *iso*-diabolic acid, mixed ether/ester lipids, soil

41

## 42 **1. Introduction**

43 Branched glycerol dialkyl glycerol tetraethers (brGDGTs) are a suite of membrane lipids that  
44 are widely used as paleoenvironmental proxies in paleoclimate studies due to their empirical  
45 relations with temperature and pH. BrGDGTs can vary in the number (4-6) and position (C-5,  
46 C-6, C-7) of methylations attached to their alkyl backbone, and can also have 0-2 internal  
47 cyclisations (Sinninghe Damsté et al., 2000; Weijers et al., 2006; De Jonge et al., 2013; Ding

48 et al., 2016). The stereochemistry of their glycerol moiety suggests that they are produced  
49 by bacteria (Weijers et al., 2006). *Acidobacteria* were proposed as likely producers due to  
50 their ubiquitous occurrence in soils and peats (Jones et al., 2009). Screening of lipid profiles  
51 of the 46 *Acidobacteria* strains that are currently available in culture indeed revealed the  
52 presence of small amounts of brGDGT-Ia in two strains from subdivision (SD) 1 (Sinninghe  
53 Damsté et al., 2011; 2014; 2018). More recently, “*Ca. Solibacter usitatus*” from SD3 was  
54 found to produce a wider variety of brGDGTs under changing temperature, oxygen, and pH  
55 conditions, albeit still not covering the entire range of brGDGTs found in the environment  
56 (Chen et al., 2022; Halamka et al., 2023).

57 Nevertheless, several strains of SD1, 3, 4, and 6 contain the membrane-spanning lipid 13, 16-  
58 dimethyl octacosanedioic acid (*iso*-diabolic acid; *iso*-DA), which has since been presumed to  
59 be a building block of brGDGTs (Sinninghe Damsté et al., 2011, 2014, 2018). Although *iso*-DA  
60 occurs ester-bound to a glycerol moiety in SD1, 3, and 6, *iso*-DA occurs as part of monoalkyl  
61 glycerol ethers (MGEs) in strains from SD4 (Sinninghe Damsté et al., 2018). Since SD4  
62 contains the gene cluster responsible for the formation of ether bonds in bacteria (i.e., *elbB*-  
63 *elbE*; Lorenzen et al., 2014), this has led to the suggestion that diether/diester lipids  
64 composed of two esterified *iso*-DA MGEs could be an intermediate compound in the brGDGT  
65 synthesis pathway (Sinninghe Damsté et al., 2018, and molecular structures therein).

66 However, the existence of mixed ether/ester-bound *iso*-DA membrane spanning lipids is  
67 merely hypothetical, as they have not yet been detected in cultures or the environment.  
68 Here we report the occurrence of tetraester and mixed ether/ester membrane-spanning  
69 lipids with a backbone consisting of *iso*-DA containing up to two additional methyl groups in  
70 mineral soils from Nepal and Rwanda. We subsequently identify the compounds released

71 after acid hydrolysis of the GDGT fractions to obtain clues on the pathway of brGDGT  
72 biosynthesis.

73

## 74 **2. Material and methods**

### 75 *2.1 Soil selection and GDGT analysis*

76 A mineral surface soil from Bremathang in Nepal (28.0768247 °N, 85.552645 °E; 3836 m  
77 above sea level (masl), pH = 4.4) was freeze dried, ground and sieved at 1 mm. Lipids were  
78 extracted by Accelerated Solvent Extraction (Dionex, ASE 350) in dichloromethane  
79 (DCM):methanol (MeOH) (9:1) with one 15 min extraction cycle. The total lipid extract (TLE)  
80 was eluted over aminopropyl using DCM:isopropanol (2:1) to obtain a neutral fraction. This  
81 fraction was further separated over a SiO<sub>2</sub> column (5% deactivated with H<sub>2</sub>O), with  
82 hydrocarbons eluting with hexane and the remainder was eluted with DCM and MeOH to  
83 obtain the GDGTs. The GDGT fraction was dissolved in hexane:isopropanol (99:1) and passed  
84 over a 0.45 µm PTFE filter. Together with the polar fraction (“extract H”) of the Rwanda soil  
85 (“soil C”) from the recent brGDGT Round Robin study (1908 masl, pH = 3.2; De Jonge et al.,  
86 2024), GDGTs were analyzed on an Agilent 1260 ultra high performance liquid  
87 chromatograph (UHPLC) coupled to an Agilent 6130 single quadrupole mass spectrometer  
88 (MS) with settings according to Hopmans et al. (2016) at Utrecht University.  
89 The Nepal polar fraction was analyzed by UHPLC - high resolution MS (HRMS) using an  
90 Agilent 1290 Infinity II equipped with thermostatted auto-injector and column  
91 compartment coupled to a Q Exactive Plus (Quadrupole Orbitrap hybrid MS) MS equipped  
92 with ion max source with APCI probe (Thermo Fisher Scientific, USA) at Royal NIOZ. Positive-  
93 ion APCI settings were as described in Baxter et al. (2019). Chromatography was as in  
94 Hopmans et al. (2016) but with the following elution method: isocratic elution for 25 min

95 with 18% B, followed by a linear gradient to 30% B at 50 min, then a linear gradient to 100%  
96 B at 80 min which was held isocratically until 120 min, where A is hexane and B is  
97 hexane:isopropanol (9:1, v/v). Flow rate was 0.2 ml min<sup>-1</sup> and the total run time was 140 min  
98 including a 20 min re-equilibration.

## 99 *2.2 Acid hydrolysis of polar fractions and analysis of released compounds*

100 Polar fractions were hydrolysed in 1.5M HCl in MeOH for 2 hours at 70 °C. After cooling, H<sub>2</sub>O  
101 and DCM were added and the organic phase was collected. The aqueous phase was  
102 extracted (2x) with DCM. The combined DCM fraction was passed over a Na<sub>2</sub>SO<sub>4</sub> column and  
103 dried under a gentle N<sub>2</sub> stream. An aliquot was methylated using  
104 trimethylsilyldiazomethane, passed over a SiO<sub>2</sub> column using ethyl acetate (EtOAc), and then  
105 silylated using *bis*(trimethylsilyl)trifluoroacetamide in pyridine at 60 °C for 20 min. The  
106 derivatised aliquots were dissolved in EtOAc and injected on-column on an Agilent 7890B  
107 gas chromatograph (GC) coupled to a 5977B MSD using a CP-sil 5CB fused silica column (30  
108 m x 0.32 mm i.d., film thickness 0.10 µm). The GC-MS was operated at a constant flow of 1.0  
109 mL min<sup>-1</sup> with helium as the carrier gas. The oven was programmed starting at 70 °C to rise  
110 to 130 °C at a rate of 20 °C min<sup>-1</sup> and then to 320 °C at a rate of 4 °C min<sup>-1</sup>, followed by an  
111 isothermal hold for 20 min. The MS was operated in Full Data Acquisition mode, scanning  
112 ions from *m/z* 50 - 800 at 70 eV. Aliquots of the polar fraction taken before and after  
113 hydrolysis were analyzed using UHPLC-MS as above, with the addition of *m/z* 1064.3,  
114 1078.3, 1092.3, 1106.3 and a window of 1.0 to the original selected ion monitoring (SIM)  
115 method.

116

## 117 **3. Results and discussion**

118 *3.1 Identification of tetraester and mixed ether/ester-bound membrane lipids in mineral soils*

119 UHPLC-MS chromatograms of the soils from Nepal and Rwanda obtained using the original  
120 settings revealed an additional peak in the  $m/z$  1050 trace, eluting at 70.4 mins, ~28 mins  
121 later than brGDGT-IIIa (Fig. 1). After screening UHPLC-MS chromatograms of soils previously  
122 analyzed at Utrecht University, the expression of this peak was tentatively linked to the low  
123 pH and/or relatively high elevation of the soils. To identify the compound represented by  
124 this peak, an accurate mass spectrum was generated using UHPLC-HRMS (Fig. 2; brGDGT-  
125 Ia+2esters). The obtained mass spectrum showed similarities with those of tetraester,  
126 tetraether, and mixed ether/ester lipids generated from cell material of different species  
127 from the order of *Thermatogales* (Sinninghe Damsté et al., 2007). Although the lipids of  
128 *Thermatogales* contain a core derived from diabolic acid rather than *iso*-DA, the close  
129 resemblance in fragmentation products with the mass spectrum generated here suggests a  
130 similar mixed ether/ester configuration of the core lipid. The exact mass of this ion at  $m/z$   
131 1049.970 indicates a  $[M+H]^+$  ion with formula  $C_{66}H_{129}O_8$ , which fits with a brGDGT-Ia in  
132 which two ethers are replaced by esters (Table 1). Notably, the HRMS spectra revealed the  
133 presence of several other compounds with comparable fragmentation patterns that,  
134 together, suggest that the soils contain membrane-spanning lipids to which the *iso*-DA  
135 backbones are attached to glycerols with one, two, or four ester bonds (Fig. 2). In addition,  
136 the *iso*-DA can have one or two additional methylations, as in brGDGT-IIa and IIIa (Fig 1,  
137 Table 1). To confirm the presence of ester bonds, aliquots of the GDGT fractions were  
138 analyzed before and after acid hydrolysis using UHPLC-MS with the addition of ions  
139 representing brGDGTs Ia, IIa, and IIIa in which all four ethers are replaced by esters to the  
140 original method, i.e.,  $m/z$  1064, 1078, 1092, and 1106. Hydrolysis resulted in the  
141 disappearance of all peaks representing the suspected tetraester and mixed ether/ester  
142 lipids in the UPLC-MS chromatogram.

143 3.2. Implications for brGDGT synthesis

144 In the soil from Nepal, three sets of Ia, IIa, and IIIa-tetraesters with virtually identical mass  
145 spectra but different retention times are present (Fig. 1; Table 1), which could be linked to  
146 the configuration of the glycerol units, or the position of the ester moiety. To possibly obtain  
147 insight in the position of the ester moieties in the mixed ether/ester lipids, the hydrolyzed  
148 GDGT fractions were analyzed using GC-MS. Interestingly, whereas hydrolysis released *iso*-  
149 DA from the Nepal GDGT fraction, this is not detected in the hydrolyzed Rwanda GDGT  
150 fraction. Instead, this fraction contains *iso*-C<sub>15</sub> and *iso*-C<sub>17</sub> MGEs, as also found in cell  
151 material from strains from SD4 (Sinninghe Damsté et al., 2014, 2018). This suggests that the  
152 mixed ether/ester lipids in these two soils could be produced by *Acidobacteria* from distinct  
153 SDs that follow different biosynthesis pathways: by tail-to-tail linkage of two *iso*-C<sub>15</sub> fatty  
154 acids to form *iso*-DA, or through the reduction of diesters into diethers and subsequent  
155 carbon-carbon linking.

156

157 **4. Conclusions**

158 The occurrence of tetraester and mixed ether/ester-bound *iso*-DA membrane-spanning lipids  
159 in the environment confirms their existence as hypothesized intermediates during brGDGT  
160 synthesis. Differences in compounds released after acid hydrolysis of the GDGT fractions  
161 support both current hypothesized biosynthesis pathways. However, both pathways contain  
162 steps for which the responsible enzymes or gene clusters have not (yet) been identified,  
163 complicating the identification of the organisms producing brGDGTs though bioinformatics.

164



165 **Acknowledgements**

166 Ellen Hopmans and Diana Sahonero Canavesi are thanked for insightful comments and  
167 Denise Dorhout for LCMS technical support. Sample collection and processing was  
168 supported with funding from US National Science Foundation Award 2021619 and 1903665.  
169 Soil was imported under USDA Permit P330-19-00164. FP acknowledges funding from NWO-  
170 Vidi grant 192.074 for experimental and analytical work.

171

172 **References**

173 Baxter, A.J., Hopmans, E.C., Russell, J.M., Sinninghe Damsté, J.S., 2019. Bacterial GMGTs in  
174 East African lake sediments: Their potential as palaeotemperature indicators. *Geochimica et*  
175 *Cosmochimica Acta* 259, 155–169.

176 Chen, Y., Zheng, F., Yang, H., Yang, W., Wu, R., Liu, X., Liang, H., Chen, H., Pei, H., Zhang, C.,  
177 Pancost, R.D., Zeng, Z., 2022. The production of diverse brGDGTs by an Acidobacterium  
178 providing a physiological basis for paleoclimate proxies. *Geochimica et Cosmochimica Acta*  
179 337, 155-165.

180 De Jonge, C., Hopmans, E.C., Stadnitskaia, A., Rijpstra, W.I.C., Hofland, R., Tegelaar, E.,  
181 Sinninghe Damsté, J.S., 2013. Identification of novel penta- and hexamethylated branched  
182 glycerol dialkyl glycerol tetraethers in peat using HPLC-MS<sup>2</sup>, GC-MS and GC-SMB-MS. *Organic*  
183 *Geochemistry* 54, 78-82.

184 De Jonge, C., Peterse, F. et al., 2024. Interlaboratory comparison of branched GDGT  
185 temperature and pH proxies using soils and lipid extracts. *Geochemistry, Geophysics,*  
186 *Geosystems* 25, e2024GC011583.

187 Ding, S., Schwab, V.F., Ueberschaar, N., Roth, V.-N., Lange, M., Xu, Y., Gleixner, G., Pohnert, G.,  
188 2016. Identification of novel 7-methyl and cyclopentanyl branched glycerol dialkyl glycerol  
189 tetraethers in lake sediments. *Organic Geochem* 102, 52-58.

190 Halamka, T.A., Raberg, J.H., McFarlin, J.M., Younkin, A.D., Mulligan, C., Liu, X.-L., Kopf, S.H.,  
191 2023. Production of diverse brGDGTs by *Acidobacterium Solibacter usitatus* in response to  
192 temperature, pH, and O<sub>2</sub> provides a culturing perspective on brGDGT proxies and  
193 biosynthesis. *Geobiology* 21, 102-118.

194 Hopmans, E.C., Schouten, S., Sinninghe Damsté, J.S., 2016. The effect of improved  
195 chromatography on GDGT-based palaeoproxies. *Organic Geochemistry* 93, 1-6.

196 Lorenzen, W., Ahrendt, T., Bozhüyük, K.A.J., Bode, H.B., 2014. A multifunctional enzyme is  
197 involved in bacterial ether lipid biosynthesis. *Nature Chemical Biology* 10, 425-427.

198 Sinninghe Damsté, J.S., Hopmans, E.C., Pancost, R.D., Schouten, S., Geenevasen, J.A.J., 2000.  
199 Newly discovered non-isoprenoid glycerol tetraether lipids in sediments. *Chemical*  
200 *Communications* 17, 1683-1684.

201 Sinninghe Damsté, J.S., Rijpstra, W.I.C., Hopmans, E.C., Schouten, S., Balk, M., Stams, A.J.M.,  
202 2007. Structural characterization of diabolic acid-based tetraester, tetraether and mixed  
203 ether/ester, membrane-spanning lipid of bacteria from the order *Thermatogales*. *Archives of*  
204 *Microbiology* 188, 629-641.

205 Sinninghe Damsté, J.S., Rijpstra, W.I.C., Hopmans, E.C., Weijers, J.W.H., Foesel, B.U.,  
206 Overmann, J., Dedysh, S.N., 2011. 13,16-dimethyl octacosanedioic acid (*iso*-Diabolic Acid), a  
207 common membrane-spanning lipid of *Acidobacteria* subdivisions 1 and 3. *Applied and*  
208 *Environmental Microbiology* 77, doi.org/10.1128/AEM.00466-11.

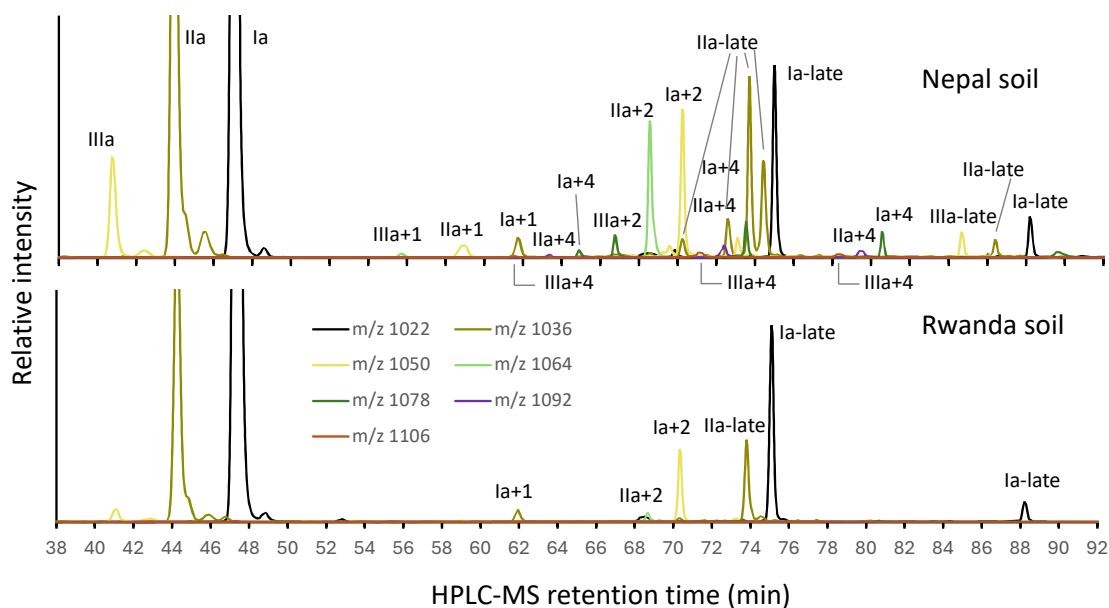
209 Sinninghe Damsté, J.S., Rijpstra, W.I.C., Hopmans, E.C., Foesel, B.U., Wüust, P.K., Overmann,  
210 J., Tank, M., Bryant, D.A., Dunfield, P.F., Houghton, K., Stott, M.B., 2014. Ether- and ester-

211 bound *iso*-Diabolic Acid and other lipids in members of *Acidobacteria* subdivision 4. Applied  
212 and Environmental Microbiology 60, doi.org/10.1128/AEM.01066-14.

213 Sinninghe Damsté, J.S., Rijpstra, W.I.C., Foesel, B.U., Huber, K.J., Overmann, J., Nakagawa, S.,  
214 Kim, J.J., Dunfield, P.F., Dedysh, S.N., Villanueva, L., 2018. An overview of the occurrence of  
215 ether- and ester-linked *iso*-diabolic acid membrane lipids in microbial cultures of the  
216 *Acidobacteria*: Implications for brGDGT paleoproxies for temperature and pH. Organic  
217 Geochem 124, 63-76.

218 Weijers, J.H.W., Schouten, S., Hopmans, E.C., Geenevasen, J.A.J., David, O.R.P., Coleman,  
219 J.M., Pancost, R.D., Sinninghe Damsté, J.S., 2006. Membrane lipids of mesophylic anaerobic  
220 bacteria thriving in peats have typical archaeal traits. Environmental Microbiology 8, 648-  
221 657.

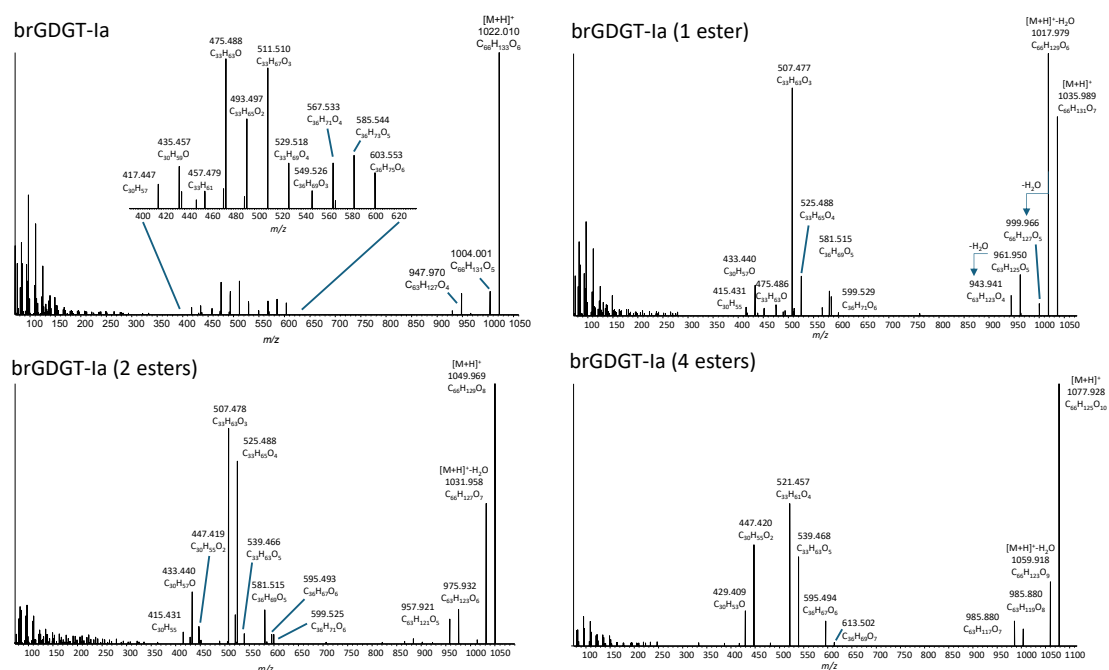
222



223

224 Figure 1. HPLC-MS chromatograms of brGDGTs in mineral soils from Nepal and Rwanda with  
 225 peaks assigned as in Table 1.

226



227

228 Figure 2. UHPLC-HRMS mass spectra of brGDGT-ia, mixed ether/ester, and tetraester-bound  
 229 *iso*-DA membrane spanning lipids in the Nepal soil based on accurate mass.

230 Table 1. Compounds observed in this study. AEC = assigned elemental composition,  $\Delta$  mmu = (measured mass – calculated mass) x 1000.

Assignment	Retention time (min) in Fig. 1	MS nominal mass ([M+H] <sup>+</sup> )	HRMS accurate mass ([M+H] <sup>+</sup> )			
			Calculated	Observed	AEC	$\Delta$ mmu
brGDGT-Ia	47.2	1022	1022.010	1022.010	C <sub>66</sub> H <sub>133</sub> O <sub>6</sub>	0.0
brGDGT-Ia late eluting	75.5	1022	1022.010	1022.012	C <sub>66</sub> H <sub>133</sub> O <sub>6</sub>	-2.0
brGDGT-Ia late eluting	88.3	1022	1022.010	1022.013	C <sub>66</sub> H <sub>133</sub> O <sub>6</sub>	-3.0
brGDGT-Ia (1 ester)	62.0	1036	1035.989	1035.991	C <sub>66</sub> H <sub>131</sub> O <sub>7</sub>	-2.0
brGDGT-Ia (2 esters)	70.4	1050	1049.968	1049.970	C <sub>66</sub> H <sub>129</sub> O <sub>8</sub>	-2.0
brGDGT-Ia (4 esters)	64.9	1078	1077.927	1077.929	C <sub>66</sub> H <sub>125</sub> O <sub>10</sub>	-2.0
brGDGT-Ia (4 esters)	73.7	1078	1077.927	1077.928	C <sub>66</sub> H <sub>125</sub> O <sub>10</sub>	-1.0
brGDGT-Ia (4 esters)	80.7	1078	1077.927	1077.931	C <sub>66</sub> H <sub>125</sub> O <sub>10</sub>	-4.0
brGDGT-IIa	45.0	1036	1036.025	1036.024	C <sub>67</sub> H <sub>135</sub> O <sub>6</sub>	1.0
brGDGT-IIa late eluting	70.7	1036	1036.025	1036.027	C <sub>67</sub> H <sub>135</sub> O <sub>6</sub>	-2.0
brGDGT-IIa late eluting	72.9	1036	1036.025	1036.028	C <sub>67</sub> H <sub>135</sub> O <sub>6</sub>	-3.0
brGDGT-IIa late eluting	73.4	1036	1036.025	1036.028	C <sub>67</sub> H <sub>135</sub> O <sub>6</sub>	-3.0
brGDGT-IIa late eluting	74.9	1036	1036.025	1036.027	C <sub>67</sub> H <sub>135</sub> O <sub>6</sub>	-2.0
brGDGT-IIa late eluting	86.4	1036	1036.025	1036.029	C <sub>67</sub> H <sub>135</sub> O <sub>6</sub>	-4.0
brGDGT-IIa (1 ester)	59.2	1050	1050.005	1050.007	C <sub>67</sub> H <sub>133</sub> O <sub>7</sub>	-2.0
brGDGT-IIa (2 esters)	69.1	1064	1063.984	1063.984	C <sub>67</sub> H <sub>131</sub> O <sub>8</sub>	0.0
brGDGT-IIa (4 esters)	63.5	1092	1091.942	1091.945	C <sub>67</sub> H <sub>127</sub> O <sub>10</sub>	-3.0
brGDGT-IIa (4 esters)	72.5	1092	1091.942	1091.945	C <sub>67</sub> H <sub>127</sub> O <sub>10</sub>	-3.0
brGDGT-IIa (4 esters)	79.6	1092	1091.942	1091.944	C <sub>67</sub> H <sub>127</sub> O <sub>10</sub>	-2.0
brGDGT-IIIa	41.1	1050	1050.041	1050.040	C <sub>68</sub> H <sub>137</sub> O <sub>6</sub>	1.0
brGDGT-IIIa late eluting	85.1	1050	1050.041	1050.044	C <sub>68</sub> H <sub>137</sub> O <sub>6</sub>	-3.0
brGDGT-IIIa (1 ester)	55.8	1064	1064.020	1064.024	C <sub>68</sub> H <sub>135</sub> O <sub>7</sub>	-4.0
brGDGT-IIIa (2 esters)	66.8	1078	1077.999	1078.002	C <sub>68</sub> H <sub>133</sub> O <sub>8</sub>	-3.0
brGDGT-IIIa (4 esters)	61.8	1106	1105.958	1105.961	C <sub>68</sub> H <sub>129</sub> O <sub>10</sub>	-3.0
brGDGT-IIIa (4 esters)	71.3	1106	1105.958	1105.959	C <sub>68</sub> H <sub>129</sub> O <sub>10</sub>	-1.0
brGDGT-IIIa (4 esters)	78.5	1106	1105.958	1105.961	C <sub>68</sub> H <sub>129</sub> O <sub>10</sub>	-3.0

231